The Journal of Experimental Biology 200, 2479–2492 (1997)
Printed in Great Britain © The Company of Biologists Limited 1997
JEB1131

CHANGING PATTERNS OF VASCULATURE IN THE DEVELOPING AMPHIBIAN RETINA

S. A. DUNLOP*, S. R. MOORE AND L. D. BEAZLEY
Department of Zoology, The University of Western Australia, Nedlands 6907, Australia

Accepted 9 July 1997

Summary

Patterns of vascularisation were examined in whole-mounted retinae from tadpole stages to adulthood in the tree frog *Litoria moorei* using perfusion with Indian ink. Changing cell densities in the underlying ganglion cell layer were studied in a parallel Cresyl-stained series. Throughout development, the vasculature was pan-retinal and the hyaloid vessel was prominent. In early tadpole stages, capillaries were arranged as a honeycomb, and their number increased at a rate sufficient to maintain high densities in the face of increasing retinal area; major arteries and veins condensed within the capillary network. By early post-metamorphic life, the retinal vasculature was remodelled by the loss of four-fifths of the capillaries; the reduction in their density was far greater than could be accounted for by continuing retinal growth. This loss resulted in a change from the honeycomb appearance to one with largely parallel vessels linked by fewer connecting ones, an arrangement that became increasingly pronounced. In post-metamorphic life, the number of branch points increased such that their density decreased only slightly in the face of considerable increases in retinal area. The density of branch points varied across the retina and changed with age. Initially, the vasculature was most dense centrally, but by mid-larval life densities were highest in two patches located in the mid-temporal and mid-nasal retina. Thereafter, the vasculature increasingly assumed gradients resembling an area centralis and visual streak, a profile that survived the vascular remodelling. The development of density gradients in the vasculature preceded that of cells in the ganglion cell layer, the latter appearing only following metamorphosis. However, in post-metamorphic life, the topographies of the retinal vasculature and cells in the ganglion cell layer were closely related.

Key words: vascularisation, tree frog, *Litoria moorei*, retina, area centralis, visual streak, development, capillary.

Introduction

Adult vertebrates display a wide range in the density distributions of neural cells within the retina, patterns that reflect the visual constraints placed on an animal by its lifestyle and environment (reviewed by Hughes, 1977; Collin, 1997). Examples of such specialised distributions include the high-cell-density fovea, the area centralis and the visual streak. The vascular demands of the outer retina are met by the choroidal circulation (Alder and Cringle, 1990; Cringle *et al.* 1990; Pournaras *et al.* 1989; Duke-Elder, 1958). Species in which the inner retina is vascularised display a wide range of blood vessel patterns which appear to be dictated by the density distributions, or topography, of neural cells in the ganglion cell layer (Michaelson, 1954; Johnson, 1968; Francois and Neetens, 1974). Capillary beds are concentrated in regions of high cell density, presumably reflecting the high metabolic demand of the latter within the neural retina. For example, in the Florida garfish *Lepisosteus platyrhincus*, the ventrally located regions of high cell density, the area centralis and visual streak, are fed by a rich capillary bed (Collin and Northcutt, 1993). A recent study examining the retinal vascular tree in the adult frog *Litoria moorei* (Tennant *et al.* 1993) confirmed earlier reports in ranid frogs (Virchow, 1881) showing a concentration of capillaries along the naso-temporal axis, which thus mirrors the topography of the area centralis and visual streak (Humphrey and Beazley, 1985). Similarly, in the adult cat *Felis domesticus*, squirrel monkey *Saimiri sciureus* and man, the area centralis and fovea are both supplied by a concentration of capillaries (Chan-Ling *et al.* 1990; Snodderly and Weinhaus, 1990; Duke-Elder, 1958). The major blood vessels differ from capillaries in that they avoid regions of high cell density. In this way, visual acuity is not compromised and, as a result of the wide variety in the topography of cells in the retinal ganglion cell layer, species display a matching variety in the patterns of their vascular trees (Copeland, 1976; Collin, 1989; Collin and Northcutt, 1993; Michaelson, 1954; Johnson, 1968; Francois and Neetens, 1974).

*e-mail: sarah@cyllene.uwa.edu.au

Development of retinal vasculature has been described only for eutherian mammals (Ashton, 1970; Shakib *et al.* 1968; Henkind and De Oliveira, 1967; Flower *et al.* 1985) and is best understood in the cat (Chan-Ling *et al.* 1990). The retinal vasculature begins to form 3 weeks before birth (gestation is 65 days) and is complete by approximately 1 month after birth, coincident with eye opening (Blakemore and Cummings, 1975), clearing of the optics (Bonds and Freeman, 1978; Thorn *et al.* 1976) and functional maturation within the primary visual system (Rusoff and Dubin, 1977; Friedlander *et al.* 1985). Despite the completion of retinal vascularisation in the cat at a time coincident with the onset of functional vision after birth, the area centralis is established almost 2 weeks before birth (Stone *et al.* 1982; Robinson, 1987), i.e. at least 5–6 weeks prior to its vascularisation (Chan-Ling *et al.* 1990).

In contrast to mammals (Rusoff and Dubin, 1977; Friedlander *et al.* 1985), the onset of visual function in amphibians occurs as early as stage 43, i.e. only 4 days after fertilization when animals emerge as free-swimming larvae (Gaze *et al.* 1974) that use visually guided behaviour for feeding and avoidance of predators. Another difference between mammals and amphibians is that, whereas cell density gradients are established early in the cat (Stone *et al.* 1982; Robinson, 1987), in amphibians these are present only from metamorphic climax as animals change from an aquatic to a terrestrial habitat (Bousfield and Pessoa, 1980; Dunlop and Beazley, 1981, 1984*a*; Coleman *et al.* 1984; Nguyen and Straznicky, 1989). Furthermore, retinal neurogenesis is complete early in mammalian development (Harman and Beazley, 1989; Harman *et al.* 1992; Rapaport and Stone, 1983; Young, 1985), but in amphibians it continues throughout life as new retinal cells are added at the ciliary margin (Straznicky and Gaze, 1971; Coleman *et al.* 1984).

Here, we have examined the structure of the vascular tree from tadpole life through to adulthood in the frog *L. moorei*. Compared with mammals, the early onset of function and the continual development of the retina in amphibians present ever-changing demands to its vascular supply. Our findings on the changing vascular tree are related to the formation of the area centralis and visual streak within the ganglion cell layer, a process reported here to match that for other amphibians (Bousfield and Pessoa, 1980; Dunlop and Beazley, 1981, 1984*a*; Coleman *et al.* 1984; Nguyen and Straznicky, 1989). Specifically, we wished to determine whether, as in adult *L. moorei*, the pattern of vasculature during development reflected the topography of cells in the ganglion cell layer. Furthermore, given the earlier onset of visual function in tadpoles compared with mammals, we investigated whether specialisations within the retinal vasculature also developed at early stages, i.e. prior to the formation of the area centralis and visual streak. Part of this work has appeared in abstract form (Dunlop *et al.* 1996).

Materials and methods

Animals and anaesthesia

Litoria moorei (Copland) at Nieuwkoop and Faber (1956) stages 47, 51, 54 and 57 were selected from a breeding colony; others were raised to metamorphic climax or to 1- to 2-month-old juveniles. There were 2- to 3-week intervals between stages 47, 51, 54 and 57, whereas only 1–2 weeks lapsed between stage 57 and metamorphic climax. We collected frogs with snout–vent lengths of 5 cm, 7 cm and 9 cm locally under license from the Department of Conservation and Land Management. The smaller frogs were approximately 1 and 2 years post-metamorphosis, respectively, and the 9 cm animals represented the largest size reported for this species, being probably at least 3–4 years old (Barker and Grigg, 1977). Animals were maintained on a 12 h:12 h L:D cycle at 22±2 °C. Pre-metamorphic stages were fed Biorell fish food and boiled lettuce; post-metamorphic animals received mealworms three times a week and were provided with water *ad libitum*. Tadpoles were killed by immersion in MS222 (0.2 % in distilled water), adults by intramuscular injection of Saffan (1.8 mg g^{-1} Alphaxalone; 0.6 mg g^{-1} Alphadolone acetate, Pittman Moore).

Preparation and analysis of tissue

Pilot studies showed that perfusion with Indian ink gave reproducible filling of the entire vascular tree. However, subsequent Cresyl staining revealed that the ink-filled vascular tree directly overlaid, and thus masked, significant numbers of cells in the ganglion cell layer (Fig. 1A,B). The retinal vasculature and density of cells in the ganglion cell layer were therefore examined using separate series of retinal whole-mounts.

Retinal vasculature

Animals were perfused intracardially with heparinised saline followed by Indian ink using a peristaltic pump. A glass micropipette was used for the young stages and a 26 gauge needle for post-metamorphic animals. Retinae (N=4 for each of the tadpole stages 47–57, N=6 at metamorphic climax, N=8 in the 1–2 month juveniles and the 5 and 7 cm frogs, and N=2 in the 9 cm adults) were dissected in saline, removing the sclera, pigment epithelium, cornea and lens. The vitreous humour was dissolved by application of hyaluronidase (Sigma), and the retina was flattened by making radial cuts, taking care not to sever major blood vessels. Retinal whole-mounts were dried onto subbed slides, dehydrated, cleared in xylene and coverslipped.

To measure retinal area, whole-mounts were viewed using a light microscope and images were frame-grabbed onto a computer at low magnification (×2) using an Optimas imaging system. Measurements were taken directly from the computer images using Optimas image-analysis software (version 4.2). For analysis of the vascular tree at pre-metamorphic stages, retinae were viewed using a light microscope, images were frame-grabbed onto a computer at high power (×20) and printed to a final magnification of ×227 to generate photomontages of the entire retina; at post-metamorphic stages, *camera lucida* drawings of the complete vascular tree were made. For each retina, all the branch points within the vascular tree were counted directly from the photomontages

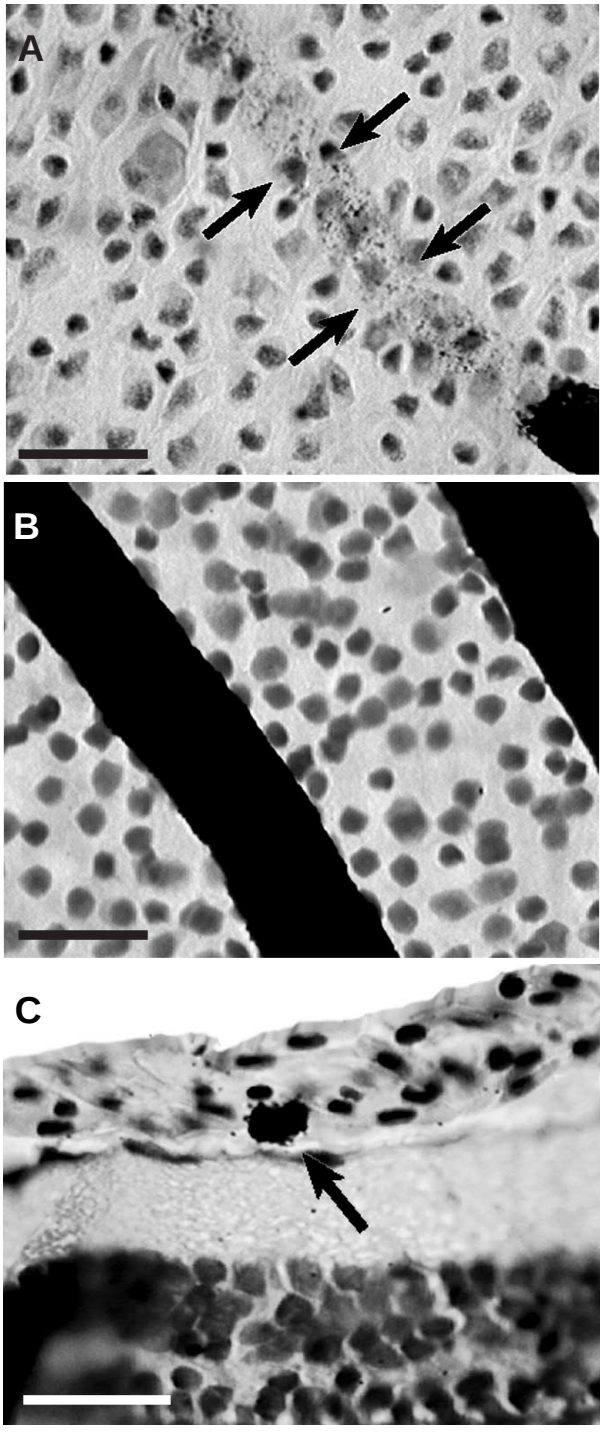

Fig. 1. (A,B) Ink-filled vessels in whole-mounts counterstained with Cresyl Violet. Incomplete filling (A) showed that vessels (black arrows) overlaid and thus obscured (B) considerable numbers of cells in the retinal ganglion cell layer. (C) Transverse retinal section (eye cup fixed with 10% buffered formalin, embedded in wax and sectioned at 10 μm) from a 9 cm adult injected with tritiated thymidine 24 h previously and processed by standard autoradiography (Coleman *et al.* 1984) showing a labelled endothelial cell within a blood vessel overlying neural retina (black arrow). Computer images were produced from frame-grabbed images (Optimas Imaging System). Contrast was increased by 15% in A–C. Scale bars, A, B, 25 μm; C, 20 μm.

and *camera lucida* drawings. The average density of branch points per mm^2 across the entire retina was also calculated by dividing the total number of branch points by the retinal area. Changes with age in retinal area, the number of branch points and the density of branch points per mm^2 were evaluated using a one-way analysis of variance (ANOVA) followed by the Fisher protected least significance difference test using Statview SE Plus Graphics software.

To examine the topography of the blood vessels, we generated isodensity maps of branch points per mm^2. The wide range in retinal area with age necessitated varying the sample size to allow sufficient sample sites per retina; these were square grids of 125 μm×125 μm at stages 47, 51 and 54, 250 μm×250 μm at stage 57 and 500 μm×500 μm from metamorphic climax onwards. For direct comparison between retinae, the numbers of branch points at these sample sites were expressed per mm^2. Furthermore, we mapped the entire population of lacunae (Burri and Tarek, 1990; Patan *et al.* 1996) and blind-ending branches (Tennant *et al.* 1993) within the capillary network. The maps were generated by scanning the photomontages of the entire retina in a serpentine fashion in adjacent but non-overlapping fields. Blind-ending branches were measured from their blood vessel of origin by aligning the vessel with a line on an eye-piece graticule and taking the measurement from that line to the tip of the branch. Using this technique, we included in the measurement the broad junction between the blind-ending branch and its parent vessel. Blind-ending vessels were included only if they were a minimum of 25 μm long. By using these criteria, we excluded small protrusions along blood vessel walls of whose identity we were uncertain.

Cells in the ganglion cell layer

A series of whole-mounts (N=2 per stage) was prepared to map cell density in the ganglion cell layer, i.e. the population of ganglion cells plus displaced amacrine cells (Humphrey and Beazley, 1985). Eyes were removed, placed in saline, dissected, treated with hyaluronidase to remove the vitreous humour as above and defatted free-floating in a series of graded alcohols, followed by treatment in xylene for 15 min. After rehydration, retinae were whole-mounted, stained with Cresyl Violet, dehydrated, cleared in xylene, coverslipped with Depex and examined at ×1000 magnification. Retinae were drawn at ×20 magnification to generate an outline on squared paper, each square having a side of 2 mm. Cells in the retinal ganglion cell layer of *L. moorei* are arranged as a monolayer and thus could be mapped accurately using whole-mount preparations. The total cell density in the retinal ganglion cell layer was counted at ×1000 using an eye-piece graticule with a side of 100 μm. The outline of the retina was used to locate regions within the sample squares and the retina thus mapped in columns and rows to cover between 1 and 4% of retinal area, the sampling frequency being highest where cell density gradients were steepest. Comparison of retinal area before and after staining revealed that shrinkage was less than 10% and

was confined to the cut edges. Post-staining retinal areas were used for our calculations.

Results

Development of vasculature and of cell topography

At stage 47, retinal area was only 2.2±0.4 mm^2 (mean ± S.D.; Fig. 2A). The ventrally located hyaloid vein was the sole major blood vessel and extended between the ventral periphery and the optic disk (Fig. 3); this vessel remained the most prominent vessel during development and adult life. There was a condensation of capillaries in the nasal retina which we assume represents the initial stages of major blood vessel formation in this quadrant. The remainder of the retina was covered by a honeycomb-like network of capillaries (Figs 3, 4A), spreading between the hyaloid vein and the peripheral collecting vessels. Small numbers of lacunae and of blind-ending vessels were seen (Figs 3, 4E–J). The topography of branch points at stage 47 (Fig. 5) was concentric, with the highest densities occurring centrally (1500 mm^{-2}) and the lowest peripherally (250 mm^{-2}). Thus, the map of the vascular tree was the reverse of that in the ganglion cell layer (Fig. 5), in which there was a shallow concentric distribution of cells with the lowest densities centrally (10×10^3 cells mm^{-2}) and the highest peripherally (15×10^3 cells mm^{-2}).

By stage 51, the retina had enlarged to 4.6±0.9 mm^2 (Fig. 2A). In addition to the prominent hyaloid vein, major blood vessels had formed both nasally and temporally (Fig. 3). Other major vessels also appeared to be in the process of condensing within the capillary bed at approximately equally spaced intervals around the radius of the retina. The honeycomb appearance of the capillary bed was maintained, and both lacunae and blind-ending branches were observed in small numbers (Fig. 3). The topography of branch points showed two zones of high density (1000 mm^{-2}), these being in the mid-temporal and mid-nasal retina (Fig. 5). Elsewhere, branch point densities had decreased somewhat compared with stage 47, at 500 mm^{-2} centrally and 250 mm^{-2} peripherally. Within the ganglion cell layer, the concentric pattern of cell topography seen at stage 47 was maintained and densities remained similar, at 10×10^3 cells mm^{-2} centrally and 16×10^3 cells mm^{-2} peripherally (Fig. 5). Therefore, regional specialisations were apparent within the vascular tree, whereas an area centralis and visual streak had not yet formed in the ganglion cell layer.

By stages 54 and 57, retinal area had increased to 7.4±3.1

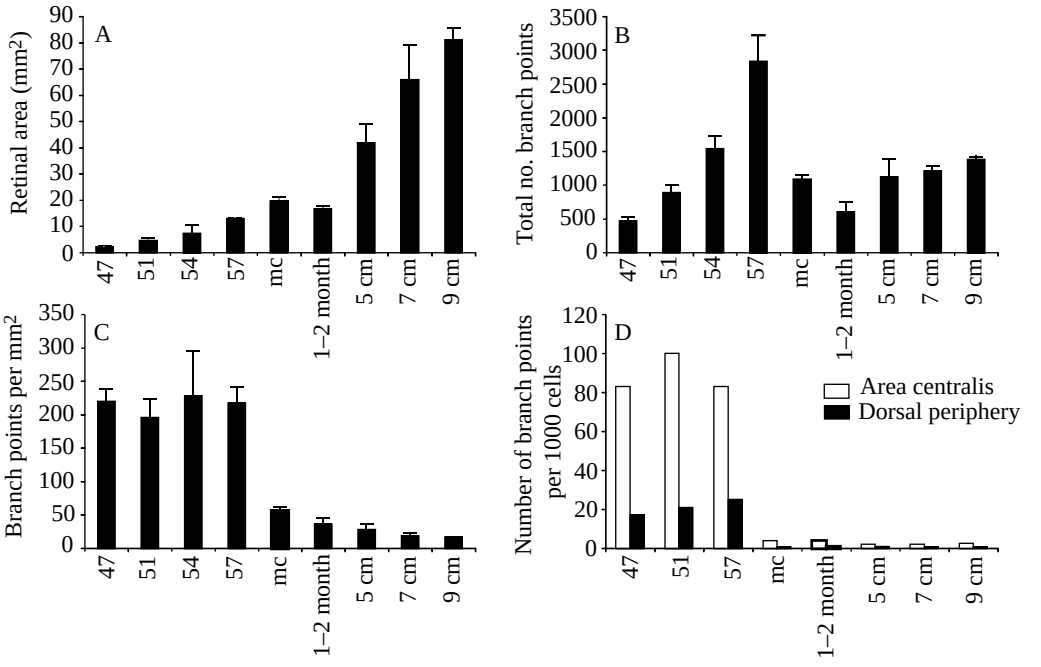

Fig. 2. Changes in retinal area (A) showed significant increases from stage 47 tadpoles to 9 cm adults (P<0.0001). Increases were significant (P<0.05) between stage 47 and 57, stage 51 and metamorphic climax (mc), stage 54 and metamorphic climax, stage 57 and 5 cm frogs, and metamorphic climax and 5 cm frogs. From 1–2 month juveniles onwards, there were significant differences (P<0.05) between the consecutive stages examined. The total number of branch points (B) showed significant changes over the stages studied (P<0.0001). Differences were significant (P<0.05) between consecutive stages up to the 5 cm frogs; thereafter, values were not significantly different (P>0.05). In addition, we calculated the number of blood vessel segments from the branch point totals using the formula $N_{bv}=2N_{bp}+1$, where N_{bv} is the number of blood vessels and N_{bp} is the number of branch points. Since the two values are directly related, the number of blood vessel segments also shows a biphasic pattern, with numbers rising during the first phase (stage 47, 945±124; stage 51, 1779±267; stage 54, 3079±363), peaking at stage 57 (5671±769), decreasing at metamorphosis (2175±113) and in the 1–2 month juveniles (1213±273) and then rising during the second, post-metamorphic phase (5 cm, 2251±511; 7 cm, 2423±147; 9 cm, 2769±75) as the retina continues to grow. The number of branch points per mm^2 (C) showed significant differences over the stages studied (P<0.0001). Values at stages 47, 51, 54 and 57 were all significantly different from those at metamorphic climax but not from each other (P<0.05). The gradual decline in values after metamorphosis was significant between metamorphic climax and the 7 cm frogs but not between the other stages. Values are means + S.D. (N=4 for stages 47–57, N=6 for metamorphic climax, N=8 for the 1–2 month juveniles and the 5 and 7 cm frogs, and N=2 for the 9 cm adults). (D) The number of branch points per 1000 cells in the ganglion cell layer for the area centralis and dorsal periphery.

and 13.0±0.3 mm^2 respectively (Fig. 2A). At least six major vessels were condensing between the central and peripheral retina (Figs 3, 6). Arteries could be distinguished from veins for the first time by a surrounding corridor approximately 50–100 μm wide which was becoming free from capillaries (Figs 3, 6), a feature maintained into maturity. The entire capillary network, however, still retained a honeycomb appearance (Figs 3, 4B, 6) and was characterised by both lacunae and blind-ending vessels (Fig. 3). The topography of blood vessel branch points showed that the two high-density patches seen at stage 51 were maintained with values of 1000–1500 mm^{-2} (Fig. 5). These patches were surrounded by a horizontally aligned band of intermediate density which ranged between 500 and 1000 mm^{-2}; densities were lowest peripherally, at 250 mm^{-2} ventrally and 100 mm^{-2} dorsally. Within the ganglion cell layer (Fig. 5), cell topography had changed to give the lowest densities in the dorsal retina (6×10^3 cells mm^{-2}) and intermediate values centrally and ventrally (10×10^3 and 12×10^3 cells mm^{-2} respectively); most notably, there was an increase in the temporal and nasal peripheries (18×10^3 cells mm^{-2}), presumably due to greater cell division at these retinal poles (Coleman *et al.* 1984). Concentrations of blood vessel branch points in the mid-temporal and mid-nasal retina were not matched by high cell densities in the ganglion cell layer.

By metamorphic climax, the retina measured 19.7±1.6 mm^2 (Fig. 2A). For the first time, arteries appeared narrower than veins and their capillary-free zone was more pronounced than at stage 57 (Fig. 3). Major vessels lay orthogonally across the horizontal axis. The honeycomb-like arrangement of capillaries had given way to a simpler, more linear arrangement of parallel vessels without numerous interconnecting capillaries, appearing as if most of the rungs of a 'ladder' had been removed (compare Fig. 4B,C). Numbers of both lacunae and blind-ending vessels had decreased to low levels (Fig. 3). The topography of blood vessel branch points showed high-density patches in the mid-temporal and mid-nasal retina but values had fallen more than 10-fold compared with stage 57, being only 100 mm^{-2} (Fig. 5). These regions were flanked by a horizontally aligned band of intermediate density with values of 50–75 mm^{-2}; densities were lowest in the dorsal and ventral peripheries, having fallen to 10 mm^{-2}. Within the ganglion cell layer (Fig. 5), an area centralis (23×10^3 cells mm^{-2}) was visible for the first time in the mid-temporal retina; there was also a high-density patch nasally (20×10^3 cells mm^{-2}) and a horizontally aligned visual streak with 16×10^3–18×10^3 cells mm^{-2}. Thus, for the first time in development, comparable specialisations were seen across the naso-temporal axis for both the vasculature and the underlying cells in the ganglion cell layer.

The major characteristics seen in the vascular tree at metamorphic climax were maintained in the 1–2 month juveniles and in the 5, 7 and 9 cm stages as retinal area continued to increase to reach 81.1±4.7 mm^2 in the 9 cm adults (Fig. 2A). The capillary bed was composed largely of parallel vessels (Fig. 4D); lacunae were not observed and the numbers of blind-ending vessels were low (Fig. 3). The streak-like topography of the vasculature appeared even more pronounced at progressively later stages (Figs 3, 7). At the area centralis, densities were 100 mm^{-2} in the 1–2 month juveniles, 50 mm^{-2} in the 5 cm frogs, 40 mm^{-2} in the 7 cm frogs and 75 mm^{-2} in the 9 cm frogs. Mid-nasally, values declined with age from 100 mm^{-2} in the 1–2 month juveniles to 75 mm^{-2} in the 5 cm frogs, 40 mm^{-2} in the 7 cm frogs and to 30 mm^{-2} in the 9 cm stage. Values across the visual streak also declined, being 50 mm^{-2} in the 1–2 month juveniles, 40 mm^{-2} in the 5 cm stage and 20 mm^{-2} in the 7 and 9 cm stages. Reductions in branch point density were also seen in the peripheral retina so that, for example, a larger region was represented by the <10 mm^{-2} isodensity line in the 9 cm than in the earlier stages.

In parallel with the streak-like arrangement of the retinal vasculature becoming more accentuated with age, so the area centralis and visual streak became more distinct in the ganglion cell layer during post-metamorphic life (Fig. 7). At the area centralis, cell densities remained high, at 23×10^3 cells mm^{-2} in the 1–2 month juveniles and the 5 cm stage, but fell slightly to 20×10^3 cells mm^{-2} in the 7 and 9 cm stages. A slight decline in density was seen in the mid-nasal retina, maximal values being 20×10^3 cells mm^{-2} in the 1–2 month juveniles, falling to 18×10^3 cells mm^{-2} in the 5 cm stage and 13×10^3 cells mm^{-2} in the 7 and 9 cm stages. Within the visual streak, values were 14×10^3 cells mm^{-2} in the 1–2 month juveniles, 13×10^3 to 15×10^3 cells mm^{-2} in the 5 cm stage and 6×10^3 to 10×10^3 cells mm^{-2} thereafter. Cell densities decreased to a greater extent with age in the dorsal and ventral peripheries from 6×10^3 cells mm^{-2} at metamorphic climax to fewer than 6×10 cells mm^{-2} in the 9 cm adult. Thus, at all post-metamorphic stages, the topography of the vasculature was mirrored by that of cells in the ganglion cell layer.

Biphasic pattern of vascular development

The above results suggest that development of the retinal vasculature is biphasic, with an early exuberant pre-metamorphic stage followed by an extensive refinement before a post-metamorphic phase of growth that is closely linked to that of the underlying retina. This interpretation was supported by comparing between stages both the total number of blood vessel branch points and the average density of branch points across the entire retina as well as changes in the relationship between the topographies of the vasculature and the cells in the ganglion cell layer.

The total number of branch points (Fig. 2B) within the vasculature showed a biphasic pattern, increasing as a result of the addition of new vessels to reach a peak at stage 57 and then decreasing as vessels were lost to a minimum at 1–2 months post-metamorphosis. Thereafter, there was a steady increase, but values never approached the pre-metamorphic peak. The total number of branch points increased steadily from 472±62 at stage 47 to 889±133 and 1539±181 at stages 51 and 54, respectively, peaking at 2835±384 at stage 57 and then declining precipitously to 1087±56 at metamorphic climax and to 606±136 in the 1–2 month juveniles (mean ± S.D.). The total

number of branch points then increased gradually to 1125±255, 1211±73 and 1384± 37 in the 5, 7 and 9 cm stages, respectively.

The average density of branch points per mm^2 also showed a biphasic pattern (Fig. 2C); values were consistently high until stage 57, fell dramatically by metamorphic climax and declined only slightly thereafter. Values were similar at 220±18 mm^{-2}, 196±28 mm^{-2}, 228±67 mm^{-2} and 217±25 mm^{-2} at stages 47, 51, 54 and 57 respectively. The maintenance of these high values despite a sixfold increase in retinal area indicated a continuous addition of new vessels to the vascular tree matching the increase in retinal area. Between stage 57 and metamorphic climax, the mean density of branch points fell fourfold to 56±5 mm^{-2}. This decline far exceeded the 1.4-fold increase in retinal area between these stages, indicating a period during which many blood vessels were removed. Had the vascular tree merely become stretched as retinal area increased, the density of branch points would have decreased by only 1.4-fold.

Mean branch point density continued to decrease to 36±9 mm^{-2}, 28±9 mm^{-2}, 19±4 mm^{-2} and 17±0 mm^{-2} in the 1–2 month juveniles and the 5, 7 and 9 cm stages, respectively. During the early part of this second phase, between the 1–2 month juveniles and the 5 cm frogs, the decline in branch point density was only slight (1.4-fold) despite a 2.5-fold increase in retinal area, indicating that, although the vascular tree was presumably being stretched by retinal growth, new blood vessels were nevertheless still being formed. Between both the 5 and 7 cm stages and the 7 and 9 cm stages, the decline in mean branch

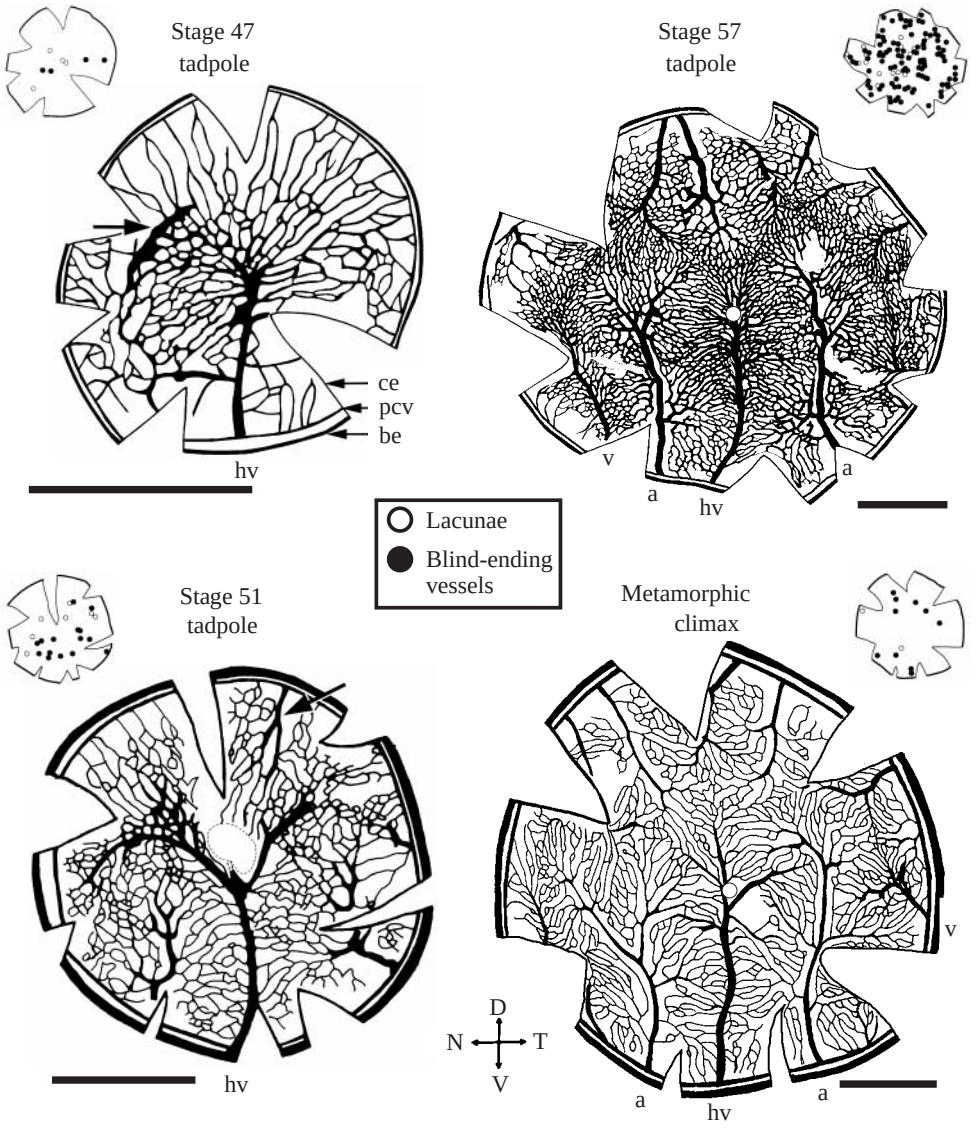

Fig. 3. *Camera lucida* drawings of the vascular tree from stage 47 tadpoles through to 9 cm adults. For ease of comparison, retinae are drawn at approximately the same size. Retinae are flattened by making a series of radial cuts around the circumference of the eye cup; a cut edge (ce) is indicated. The biological edge (be) of the retina is shown by the thick, outermost line; the thin inner line represents the peripheral collecting vessels (pcv). The arrow in the stage 47 retina indicates an example of a major vessel condensing from within the central region of the capillary bed. The arrow in the stage 51 retina indicates an example of a major vessel condensing at the periphery of the capillary bed. The major

point density (1.4-fold and 1.1-fold, respectively) approximately balanced the increase in retinal area (1.5-fold and 1.2-fold, respectively), indicating that branch points were added at a rate that matched the continuing expansion of the retina.

The biphasic nature of vascular development was also shown by the changes in the number of blood vessel branch points relative to the number of cells in the ganglion cell layer (Fig. 2D). Two retinal regions were considered, the mid-temporal retina and the dorsal periphery, destined to become the regions of highest cell density, the area centralis, and of lowest cell density, respectively. Using data from the representative isodensity maps (Figs 5, 7), we calculated the number of branch points per 1000 cells in these regions (Fig. 2D). For the area centralis, values were highest up to stage 57 at 83–100 branch points per 1000 cells, decreased 20-fold to 4 branch points per 1000 cells by metamorphic climax and then declined to 2.5 per 1000 cells by the 9 cm stage. In the dorsal periphery, values were also highest up to stage 57, being 17–25 per 1000 cells and also decreased 20-fold by metamorphic climax to a value of 0.8 per 1000 cells which was maintained thereafter.

Discussion

The pattern of retinal vasculature in the frog *L. moorei* reflects the topography of cells in the ganglion cell layer

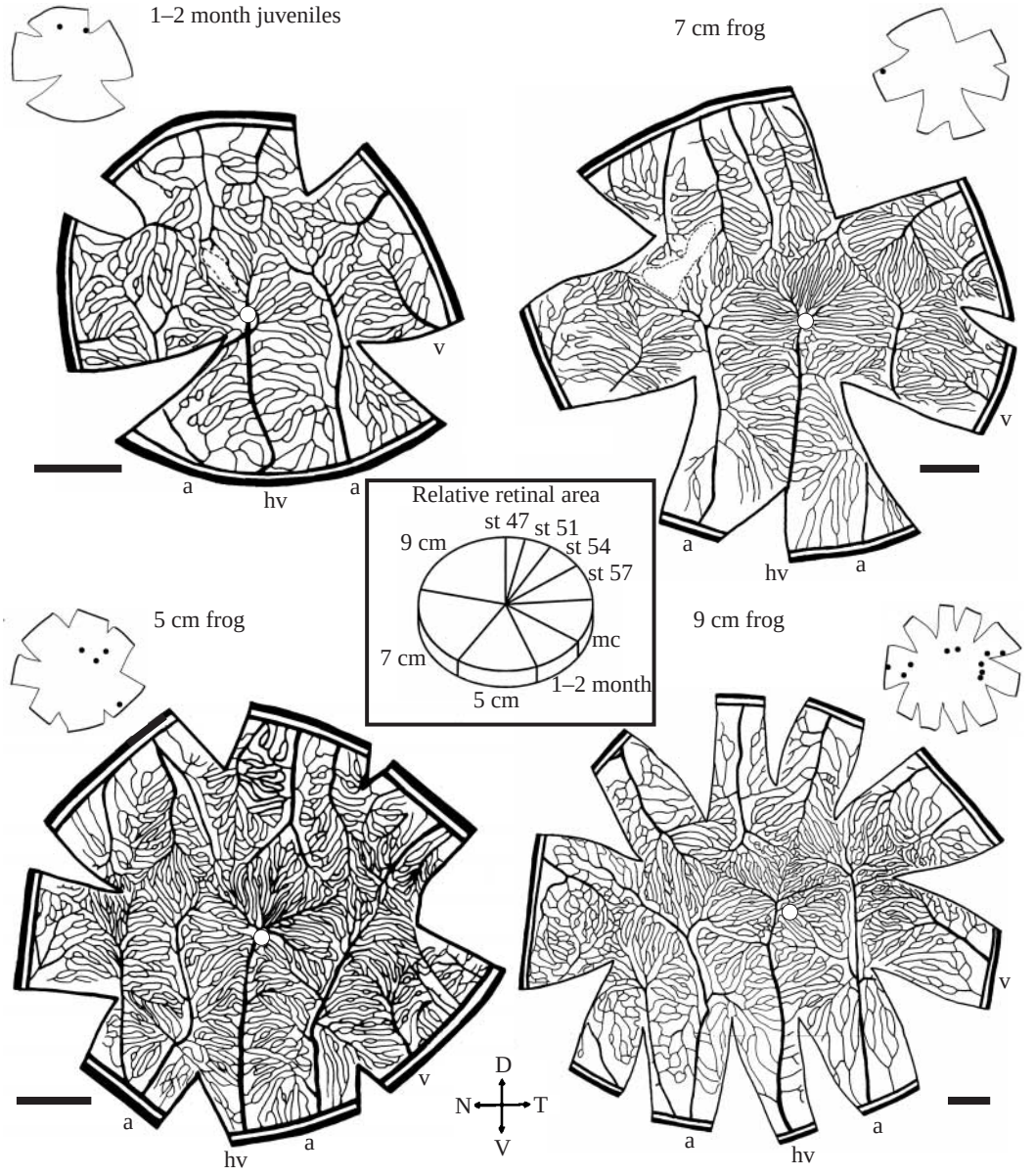

ventrally located hyaloid vein (hv) is indicated throughout. Arteries (a) are distinguished from veins (v) by their adjacent capillary-free zone. The position of the optic disk is indicated by a small white disk in the central retina. Small holes in the retina produced during the mounting procedure are outlined by broken lines. Insets for each retina show maps of the total population of lacunae (open circles) and blind-ending vessels (filled circles) associated with the capillary bed. D, V, N and T are dorsal, ventral, nasal and temporal, respectively. The pie-slice diagram indicates relative retinal area for the stages examined. st, developmental stage; mc, metamorphic climax. Scale bars are 1 mm throughout.

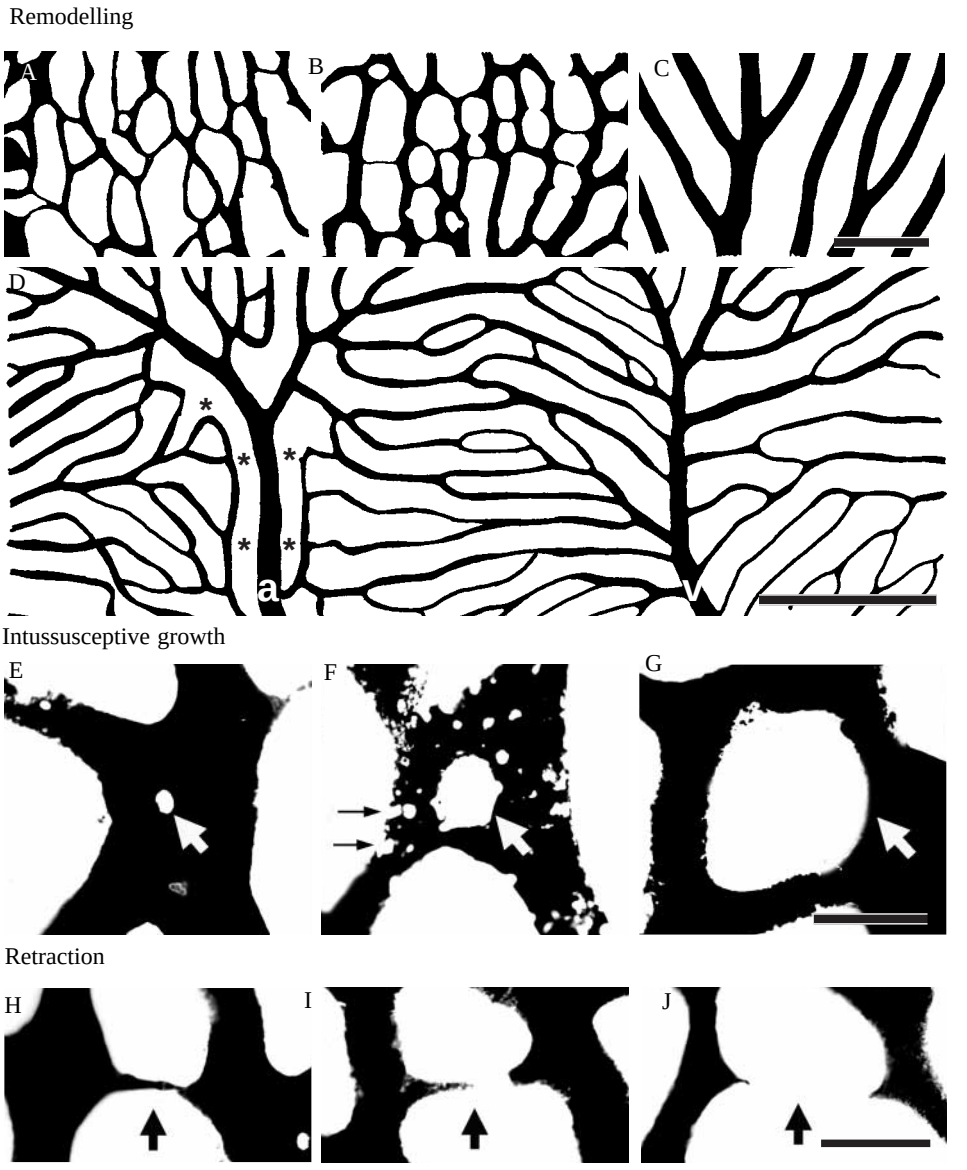

Fig. 4. (A-D) *Camera lucida* drawings of the capillary bed at stage 47 (A), stage 57 (B) and in the 9 cm frog (C). The honeycomb appearance in the youngest stages gives way to a largely linear arrangement of blood vessels after metamorphosis. In the adult (D) and from metamorphic climax onwards, arteries (a) are thicker than the veins (v) and are surrounded by a capillary-free zone (indicated by asterisks). (E–J) Photomicrographs of ink-filled capillary beds. (E-G) Capillary junctions in a stage 57 tadpole showing lacunae (white arrows), the hallmark of intussusceptive growth (Burri and Tarek, 1990; Patan *et al.* 1996), indicative of progressive stages in the formation of a capillary branch point. The white speckled appearance of the vessels in F (small black arrows) is due to non-adherence of ink to the inside of the vessels. (H–J) Blind-ending capillary branches in a stage 57 tadpole suggestive of a sequence of capillary retraction (arrows). The late onset of blood flow in capillaries that form by budding suggests that blind-ending branches are not newly forming; had they been so, they could not have been filled with ink. They are probably remnants of patent capillaries that are regressing. The photomicrographs in E–J were produced from black-and-white negative film using a Hewlett Packard Scan Jet S4c/T scanner together with Photoshop and Page Maker image-processing programs. Contrast was increased by 15 %. Scale bars, A–C, 20 μm; D, 500 μm; E–G, 25 μm; H–I, 30 μm.

throughout development. Furthermore, specialisations within the retinal vasculature appear before the emergence of the area centralis and visual streak. The retinal vasculature develops in two distinct phases. The first takes place pre-metamorphically as the retina enlarges, and the second occurs post-metamorphically against a backdrop of continuing increases in retinal area. During the first phase, a continuous addition of blood vessels maintains their high density and a topography emerges which resembles an area centralis and visual streak. However, comparable specialisations do not begin to form amongst the underlying cells in the ganglion cell layer until later, i.e. by metamorphic climax. By the end of the first phase, the vasculature is remodelled by the removal of numerous blood vessels, although the specialised topography remains intact. During the second phase, the addition of new blood vessels ensures that their density falls only slightly as the retina continues to grow. The topography of blood vessels becomes accentuated with age as does that of the area centralis and visual streak in the ganglion cell layer.

Development of retinal vasculature

The functional integrity of neural tissue is critically dependent on an appropriate vascular supply and, during development, numerous factors probably influence vascularisation. A major factor is oxygen levels, with high metabolic demand driving the formation of new vessels and low demand resulting in vessel retraction (Michaelson, 1948; Ashton, 1966; Ashton and Pedler, 1962; Weiter *et al.* 1981; Phelps, 1990; Rosen *et al.* 1991; Chan-Ling *et al.* 1992, 1995).

Initial vascularisation

The vertebrate retina is initially vascularised by hyaloid vessels which enter the ventrally located optic fissure shortly after invagination of the optic cup (Mann, 1964; Grant *et al.*

1980). In some fish and amphibians, the hyaloid system persists, spreading as a monolayer apposed to the ganglion cell layer to give rise to the retinal vessels. In contrast, the developing mammalian retina is supplied only transiently by the hyaloid vein (Duke-Elder, 1958), with the ophthalmic vessels arising later and becoming embedded within the ganglion cell layer. The factors that control the persistence or regression of the hyaloid system have yet to be determined. However, before stage 47 in *L. moorei*, retinal thickness is approximately 200 μm (Grant *et al.* 1980; Dunlop and Beazley, 1984*b*) and thus greater than the theoretical maximum of 140 μm for oxygen diffusion from the choroidal supply (Chase, 1982; Dunlop *et al.* 1994). At the earliest larval stages in amphibians, it is likely that a high oxygen demand stimulates the transition of the hyaloid into the retinal circulation.

The formation of capillaries

By the first stage at which we could examine the vasculature in *L. moorei* (stage 47), a pan-retinal capillary supply was evident. A process likely to underlie its formation is sprouting

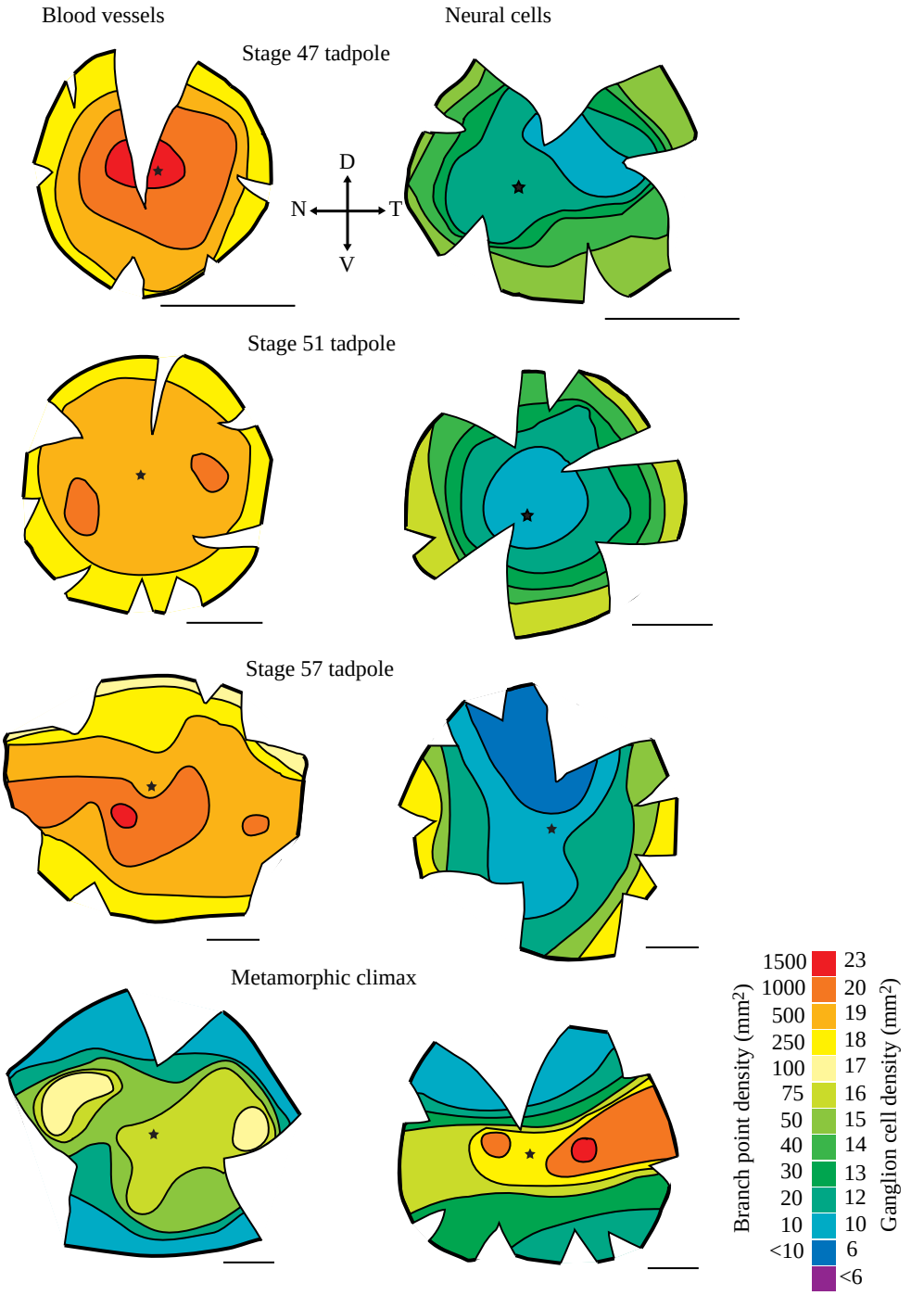

Fig. 5. Retinal whole-mounts from stage 47 to metamorphic climax showing isodensity maps of branch point density per mm^2 (left panel) and, for a whole-mounts from animals of equivalent age, isodensity maps of the neural cell density in the retinal ganglion cell layer (right panel). A star indicates the position of the optic nerve head. D, V, N and T are dorsal, ventral, nasal and temporal, respectively. Scale bars, 1 mm throughout.

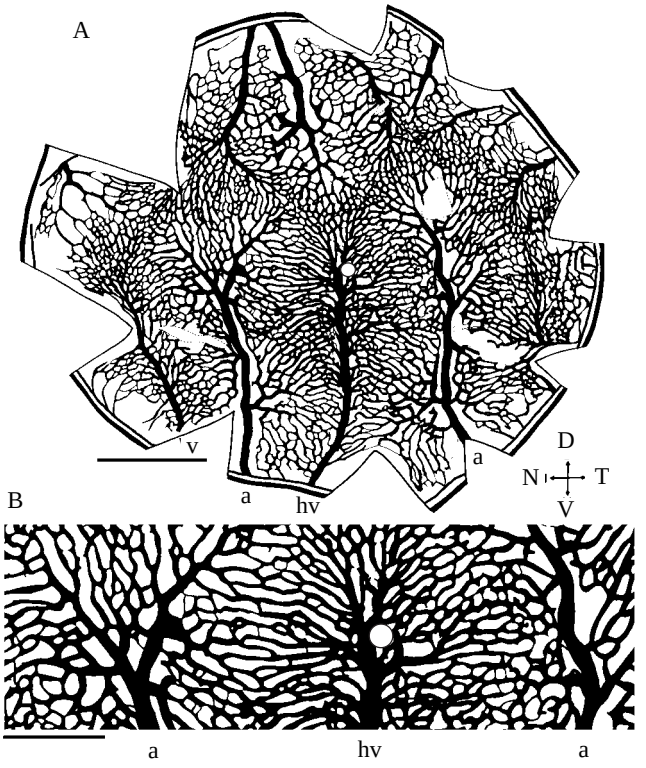

Fig. 6. (A) *Camera lucida* drawing of the vascular tree at stage 57; (B) details of the capillary bed across the central part of the naso-temporal axis. D, V, N and T are dorsal, ventral, nasal and temporal, respectively. a, artery; v, vein; hv, hyaloid vein. Scale bars, A, 1 mm; B, 500 μm.

angiogenesis, also termed capillary budding, in which new vessels sprout from existing ones by the temporary breakdown of capillary walls followed by the migration and alignment of newly generated endothelial cells; the sprouts anastomose and only then do the vessels become patent (Folkman, 1985; Risau, 1997). In mammals, development of the ophthalmic vessels takes place by a different sequence of events. There are two processes (Ashton, 1970; Shakib *et al.* 1968; Henkind and De Oliveira, 1967; Flower *et al.* 1985), best documented in the cat (Chan-Ling *et al.* 1990). In the first, mesenchymal spindle cells invade the eye *via* the optic disk, migrate across the retina and become transformed into blood vessels within the ganglion cell layer. The now pan-retinal ophthalmic vessels undergo capillary budding to supply the deeper retinal layers, a process that starts at the area centralis and spreads peripherally.

Once the capillary bed is established in *L. moorei*, there is a pan-retinal addition of blood vessels during the first phase of vascularisation which maintains their density in the face of increasing retinal area. We are uncertain which process is responsible for the addition of blood vessels, although it is unlikely that spindle cell migration and transformation occur. At no stage in our Cresyl-stained whole-mounts could we detect the long, radially oriented spindle cells that in the cat were closely associated with the nerve fibre layer (Chan-Ling *et al.* 1990). Furthermore, in *L. moorei*, the entire retina was already covered by the vascular network, whereas in the cat blood vessels form in a strict centre-to-periphery gradient.

A different process of capillary formation, termed non-sprouting angiogenesis or intussusceptive growth, has not previously been reported in the retina but has been described in foetal mammalian lung and chick chorio-allantoic membrane (Burri and Tarek, 1990; Patan *et al.* 1996; Risau, 1997). Existing capillaries are divided by the insertion of pillars of tissue or lacunae which, as they expand, take on the appearance of a new mesh within a capillary bed. We have evidence of intussusceptive growth within the retina of *L. moorei* in that lacunae were observed during the first, but not the second, phase of vascular development (see Fig. 3). The small number of lacunae may indicate that their expansion to a branched capillary occurs rapidly, thus underlying the addition of many vessels. Alternatively, intussusceptive growth may give rise to only a proportion of new blood vessels and, if so, the vasculature must also expand by capillary budding. During the second phase, the vasculature is presumably growing solely by capillary budding, a suggestion supported by the slight but steady increase in the total number of branch points. Indeed, pilot data using tritiated thymidine autoradiography to label dividing cells (Fig. 1C) have shown that mitosis occurs within the vasculature even in the 9 cm adults.

In amphibians, the retinal vessels remain as a monolayer and are thus unlike those of eel-fishes (Hanyu, 1959) or some species of mammal in which one or more layers of capillaries bud off into the deeper retinal layers (Engerman and Meyer, 1965; Chan-Ling *et al.* 1990; McMenamin and Krause, 1993; Snodderly and Weinhaus, 1990). The stimulus for the formation of additional capillary beds must be absent from the amphibian retina. In mammals, the overlap between capillary beds and high levels of cytochrome oxidase staining suggests a correlation between retinal vasculature and functional demand (Kageyama and Wong-Riley, 1984; Snodderly and Weinhaus, 1990) rather than retinal thickness *per se* (Chase, 1982).

Remodelling the capillary bed

During the final part of the first phase of retinal vascularisation in *L. moorei*, the density of blood vessels declines dramatically, although the major vessels stay intact. As in the developing cat retina (Chan-Ling *et al.* 1990), capillaries in *L. moorei* appear to be removed actively by a degenerative process in which the lumen narrows and finally collapses. The highest number of blind-ending vessels, considered to represent degenerating capillaries, is seen at stage 57 before the precipitous decline in blood vessel numbers by metamorphic climax. Thyroxine is an essential trigger during metamorphosis for the degeneration of many tissues including the gut and respiratory surfaces, both of which are highly vascularised (Fox, 1983). An investigation using *in situ* labelling of endogenous endonuclease activity associated with programmed cell death (Gavrieli *et al.* 1992) would identify degenerating endothelial cells and determine the extent of cell death during this process. In addition, thyroxine also triggers

changes in haemoglobin structure such that the oxygen-carrying capacity of blood increases from 7 volume % in larvae to 11 volume % in adults (Fox, 1983). Presumably, the lower blood vessel densities in the second phase are in part compensated by the greater oxygen-carrying capacity of the adult form of haemoglobin. The small numbers of blind-ending vessels after metamorphic climax suggest that only limited vessel degeneration takes place in the maturing vasculature.

A different pattern of exuberance and remodelling from that seen in *L. moorei* has been reported in the cat (Chan-Ling *et al.* 1990). Exuberance is confined to the leading edge of the vasculature, where spindle cells transform into the capillary plexus. More centrally, vessels have matured, presumably already pruned of excess capillaries. However, the absence of exuberance and remodelling from the developing vasculature which supplies the deeper retinal layers in the cat illustrates that remodelling is not essential for establishing all mature vascular beds.

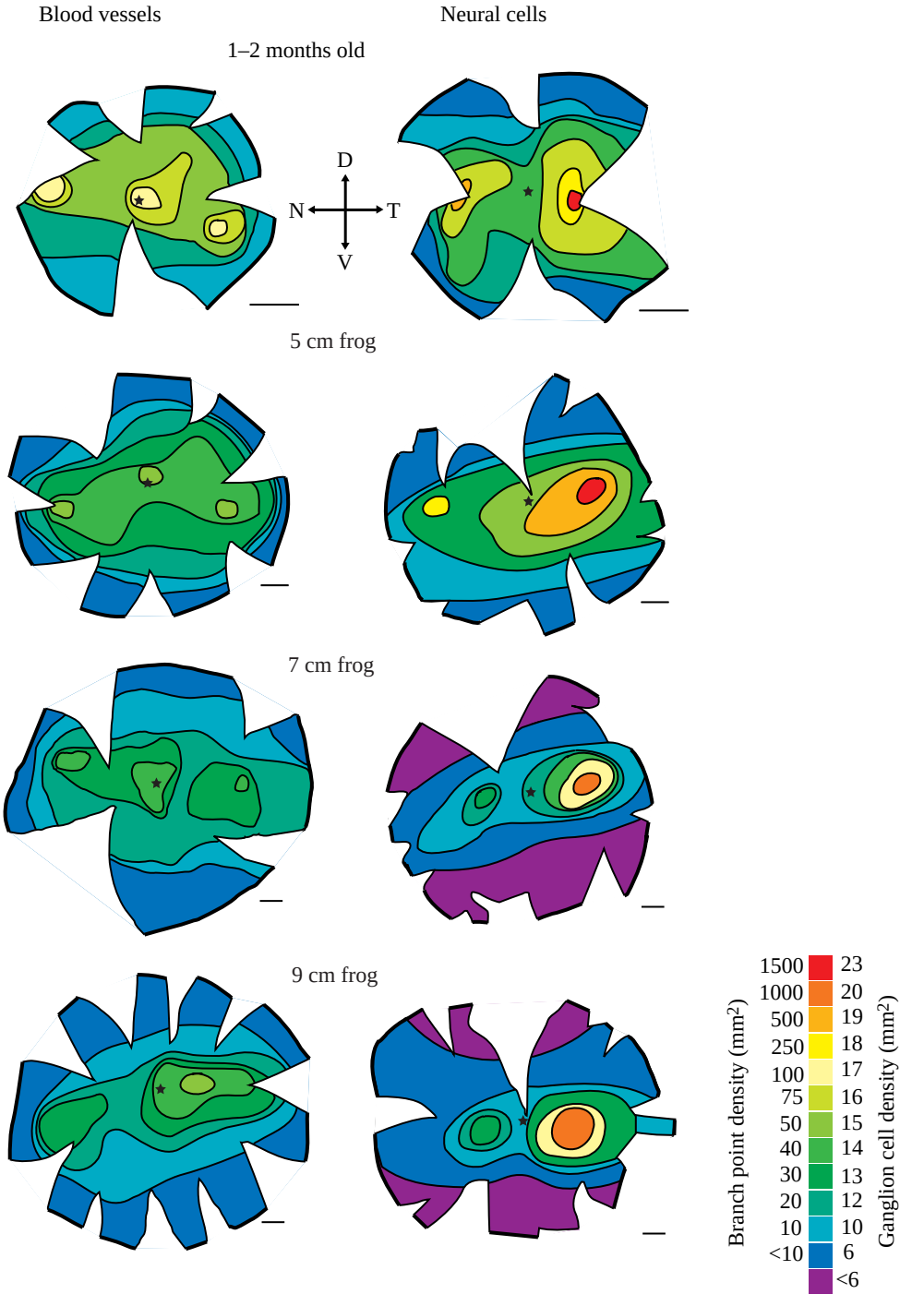

Fig. 7. Retinal whole-mounts from 1–2 month juveniles to 9 cm frogs showing isodensity maps of branch point density per mm^2 (left panel) and, for whole-mounts from animals of equivalent ages, isodensity maps of the neural cell density in the retinal ganglion cell layer (right panel). A star indicates the position of the optic nerve head. D, V, N and T are dorsal, ventral, nasal and temporal, respectively. Scale bars, 1 mm throughout.

Growth of the vascular tree and continuing increases in retinal area

In *L. moorei*, a process must occur whereby the post-metamorphic vascular tree is expanded with increasing retinal area. Expansion of the retina is pronounced in the second phase of vascular development, and it presumably triggers the rise in the total number of branch points. However, the slight but continuing decline in branch point density with post-metamorphic age indicates that the growth of the vasculature is outstripped by that of the retina itself. Within the area centralis and across the naso-temporal axis, growth of new blood vessels must, however, match that of the neural retina since a high concentration of blood vessels is maintained within this region. Elsewhere, for example in the dorsal periphery, the density of blood vessels decreases. In mammals, the retina grows non-uniformly (Mastronarde *et al.* 1984; Sengelaub *et al.* 1986; Lia *et al.* 1987; McCall *et al.* 1987; Robinson, 1987; Robinson *et al.* 1989). Although the mechanisms that drive such growth are unclear (Coulombre, 1956; Liu *et al.* 1986), the retinal vasculature presumably undergoes a similar asymmetric expansion.

Major vessels

Major vessels are considered to condense from capillaries (Folkman, 1985). In *L. moorei*, some vessels appear from the centre outwards while others originate from the peripheral collecting vessels (see Fig. 3), which together results in arteries and veins being equally spaced around the retinal circumference. In the cat, the pattern differs from that of *L. moorei*, with condensation occurring within a trilobed capillary bed giving rise to the three main artery–vein pairs (Chan-Ling *et al.* 1990) which radiate from the optic disk (Hughes, 1975).

The factors which drive the condensation of major vessels must vary widely between species to result in the strikingly different vascular trees that are observed within the vertebrates (Johnson, 1968; Michaelson, 1954; Francois and Neetens, 1974). Furthermore, an absence of major vessels within the deeper retinal layers of mammals (Chan-Ling *et al.* 1990) suggests that such factors also vary between retinal layers. It is possible that in amphibians, as in the cat, interactions with the underlying nerve fibre layer are important in determining the arrangement of major blood vessels. In the cat, spindle cells migrate across the nerve fibre layer, avoiding the presumptive area centralis from as early as embryonic day 29 (Chan-Ling *et al.* 1990). The cells seem able to avoid this region prior to the appearance of cell density gradients at embryonic day 54 (Lia *et al.* 1987; Robinson, 1987). Spindle cells may follow axons in the arcuate raphe, an arrangement that, in primates, is present before the inception of the fovea (Steineke and Kirby, 1993). In amphibians, the development of the area centralis and visual streak by metamorphic climax and the accentuation of these specialisations thereafter suggest that dynamic interactions between the vasculature and the neural retina continue throughout life.

The vascular tree and metabolic demand of the retina

During the first phase in *L. moorei*, the overall density of the retinal vasculature is higher than subsequently, although cell densities are within the adult range. Presumably, the high density of blood vessels is necessary to serve the greater demands of immature cells which are completing mitosis and migration, elaborating axons and dendrites and establishing functional synaptic connections (Grant *et al.* 1980; Holt, 1989; Frank and Hollyfield, 1987; Gaze *et al.* 1974). Moreover, these events follow a centro-peripheral gradient (Straznicky and Gaze, 1971). The high density of blood vessels in the central retina by stage 47 presumably reflects a higher metabolic activity in this more developmentally advanced region than in the peripheral retina, even though cell densities are greater peripherally than centrally.

At stage 51 and 57, there are two high-density patches of vasculature within the mid-temporal and mid-nasal retina which appear several weeks before the area centralis and visual streak and may indicate a locally raised oxygen demand. Because the retina grows continually at its edge (Straznicky and Gaze, 1971; Coleman *et al.* 1984), the area centralis and visual streak will form in regions peripheral to the two high-density vascular patches. These patches may act as a source of endothelial cells which seed newly forming capillaries as the area centralis and visual streak form within the ganglion cell layer. This chronological sequence ensures that the area centralis and visual streak will be highly vascularised, and therefore able to function, as soon as they are formed. In contrast, in the cat, the formation of capillaries at the area centralis is complete only by postnatal day 28 (Chan-Ling *et al.* 1990), i.e. 5–6 weeks after it can be identified by cell density gradients (Lia *et al.* 1987; Robinson, 1987). In *L. moorei*, therefore, vascularisation occurs before the area centralis forms, whereas in the cat the area centralis forms before its capillary bed. Nevertheless, in both *L. moorei* and the cat, the area centralis is vascularised from the onset of functional vision.

From metamorphic climax onwards, it is clear that the density of blood vessels in frog retinae is directly related to neural cell density. However, the density of the vasculature per 1000 cells is greater at the area centralis than at the dorsal periphery. The difference suggests that each cell in the area centralis imposes a greater metabolic load than its counterpart in the peripheral retina. We do not yet understand the retinal distribution of the numerous ganglion cell types present in the amphibian retina (Frank and Hollyfield, 1987). It may be that those with the highest metabolic demand are found in the area centralis whilst those cells with lower metabolic demands dominate more peripheral regions.

S.A.D. is a Research Fellow, National Health and Medical Research Council (NH&MRC, Australia). We thank W. M. Ross, R. Roberts and T. Moroney for expert technical assistance and Dr J. D. Roberts for statistical advice. This work was funded by the NH&MRC.

References

ALDER, V. A. AND CRINGLE, S. J. (1990). Vitreal and retinal oxygenation. *Graefe's Arch. clin. exp. Ophthalmol*. **228**, 151–157.

ASHTON, N. (1966). Oxygen and the growth and development of retinal vessels: *In vivo* and *in vitro* studies. *Am. J. Ophthalmol*. **62**, 412–435.

ASHTON, N. (1970). Retinal angiogenesis in the human embryo. *Br. Med. Bull.* **26**, 103–106.

ASHTON, N. AND PEDLER, C. (1962). Studies on developing retinal vessels. IX. Reaction of endothelial cells to oxygen. *Br. J. Ophthalmol*. **46**, 257–276.

BARKER, J. AND GRIGG, G. (1977). *A Field Guide to Australian Frogs.* Perth, Sydney: Rigby Ltd.

BLAKEMORE, C. AND CUMMINGS, R. M. (1975). Eye opening in kittens. *Vision Res.* **15**, 1417–1418.

BONDS, A. B. AND FREEMAN, R. D. (1978). Development of optical quality in the kitten eye. *Vision Res*. **18**, 391–398.

BOUSFIELD, J. D. AND PESSOA, V. F. (1980). Changes in ganglion cell density during post-metamorphic development in a neotropical tree frog *Hyla raniceps*. *Vision Res.* **20**, 501–510.

BURRI, P. H. AND TAREK, M. R. (1990). A novel mechanism of capillary growth in the rat pulmonary microcirculation. *Anat. Rec*. **228**, 35–45.

CHAN-LING, T.-L., GOCK, B. AND STONE, J. (1995). The effect of oxygen on vasoformative cell division. Evidence that 'physiological hypoxia' is the stimulus for normal retinal vasculogenesis. *Invest. Ophthalmol. Vis. Sci.* **36**, 1201–1214.

CHAN-LING, T.-L., HALASZ, P. AND STONE, J. (1990). Development of retinal vasculature in the cat: processes and mechanisms. *Curr. Eye Res*. **9**, 459–478.

CHAN-LING, T.-L., TOUT, S., HOLLANDER, H. AND STONE, J. (1992). Vascular changes and their mechanisms in the feline model of retinopathy of prematurity. *Invest. Ophthalmol.* **33**, 2128–2147.

CHASE, J. (1982). The evolution of retinal vascularization in mammals: a comparison of vascular and avascular retinae. *Ophthalmology* **89**, 1518–1525.

COLEMAN, L.-A., DUNLOP, S. A. AND BEAZLEY, L. D. (1984). Patterns of cell division during visual streak formation in the frog *Limnodynastes dorsalis*. *J. Embryol. exp. Morph.* **83**, 119–135.

COLLIN, S. P. (1989). Topographic organisation of the ganglion cell layer and intraocular vascularisation in the retinae of two reef teleosts. *Vision Res.* **29**, 765–775.

COLLIN, S. P. (1997). Behavioural ecology and retinal cell topography. In *Adaptive Mechanisms in the Ecology of Vision* (ed. S. N. Archer, M. B. A. Djamgoz, E. Loew, J. C. Partridge and S. Vallerga). London: Chapman & Hall (in press).

COLLIN, S. P. AND NORTHCUTT, R. G. (1993). The visual system of the Florida garfish, *Lepisosteus platyrhincus* (Ginglymoidi). *Brain Behav. Evol.* **42**, 295–320.

COPELAND, D. E. (1976). The anatomy and fine structure of the eye in teleosts. IV. The choriocapillaris and the dual vascularisation of the area centralis in *Fundulus grandis*. *Exp. Eye Res.* **22**, 169–179.

COULOMBRE, A. J. (1956). The role of intraocular pressure in the development of the chick eye. *J. exp. Zool.* **133**, 211–225.

CRINGLE, S. J., YU, D.-Y. AND ALDER, V. A. (1991). Intraretinal oxygen tension in the rat eye. *Graefe's Arch. clin. exp. Ophthalmol.* **239**, 1–4.

DUKE-ELDER, SIR, S. (1958). *System of Ophthalmology*, vol. 11, chapter. 2. London: Kimpton.

DUNLOP, S. A. AND BEAZLEY, L. D. (1981). Changing retinal ganglion cell distribution in the frog *Heleioporus eyrei*. *J. comp. Neurol.* **202**, 221–236.

DUNLOP, S. A. AND BEAZLEY, L. D. (1984*a*). A morphometric study of the retinal ganglion cell layer and optic nerve from metamorphosis in *Xenopus laevis*. *Vision Res*. **24**, 417–427.

DUNLOP, S. A. AND BEAZLEY, L. D. (1984*b*). Cell distributions in the retinal ganglion cell layer of adult Leptodactylid frogs after premetamorphic eye rotation. *J. Embryol. exp. Morph*. **89**, 159–173.

DUNLOP, S. A., MOORE, S. M., TENNANT, M. AND BEAZLEY, L. D. (1996). Development of retinal vasculature in the frog *Litoria moorei*. *Proc. Aust. physiol. pharmac. Soc*. **27**, 37P.

DUNLOP, S. A., ROSS, W. M. AND BEAZLEY, L. D. (1994). The retinal ganglion cell layer and optic nerve in a marsupial, the honey possum (*Tarsipes rostratus*). *Brain Behav. Evol*. **44**, 307–323.

ENGERMAN, R. L. AND MEYER, R. K. (1965). Development of retinal vasculature in rats. *Am. J. Ophthalmol.* **60**, 628–641.

FLOWER, R. W., MCLEOD, D. S., LUTTY, G. A., GOLDBERG, B. AND WAJER, S. D. (1985). Postnatal retinal vascular development of the puppy. *Invest. Ophthalmol. Vis. Sci.* **26**, 957–968.

FOLKMAN, J. (1985). Tumour angiogenesis. *Adv. Cancer Res.* **43**, 175–203.

FOX, H. (1983). *Amphibian Morphogenesis*. Clifton, NJ: Humana Press.

FRANCOIS, J. AND NEETENS, A. (1974). Comparative anatomy of the vascular supply of the eye in vertebrates. In *The Eye*, vol. 5, *Comparative Physiology* (ed. H. Davson and L. T. Graham), pp. 1–70. New York: Academic Press.

FRANK, B. D. AND HOLLYFIELD, J. G. (1987). Retina of the tadpole and frog: Delayed dendritic development in a subpopulation of ganglion cells coincident with metamorphosis. *J. comp. Neurol.* **296**, 435–444.

FRIEDLANDER, M. J., MARTIN, K. C. AND VAHLE-HINZ, C. (1985). The structure of the terminal arborisation of physiologically identified retinal ganglion cell axons in the kitten. *J. Physiol., Lond*. **359**, 293–313.

GAVRIELI, Y., SHERMAN, Y. AND BEN-SASSON, S. A. (1992). Identification of programmed cell death *in situ via* specific labelling of nuclear DNA fragmentation. *J. Cell Biol.* **119**, 493–501.

GAZE, R. M., KEATING, M. J. AND CHUNG, S.-H. (1974). The evolution of the retinotectal map during development in *Xenopus laevis*. *Proc. R. Soc. Lond. B* **185**, 301–330.

GRANT, P., RUBIN, E. AND CIMA, C. (1980). Ontogeny of the retina and optic nerve in *Xenopus laevis*. I. Stages in the early development of the retina. *J. comp. Neurol*. **189**, 593–613.

HANYU, I. (1959). On the falciform process, vitreal vessels and other related structures of the teleost eye. I. Various types and their interrelationship. *Bull. Jap. Soc. Scientific Fisheries* **25**, 595–613.

HARMAN, A. M. AND BEAZLEY, L. D. (1989). Generation of retinal cells in the wallaby, *Setonix brachyurus*. *Neuroscience* **28**, 219–232.

HARMAN, A. M., SANDERSON, K. J. AND BEAZLEY, L. D. (1992). Biphasic retinal neurogenesis in the brush-tailed possum, *Trichosurus vulpecula*: Further evidence for the mechanisms involved in formation of ganglion cell density gradients. *J. comp. Neurol.* **325**, 595–606.

HENKIND, P. AND DE OLIVEIRA, L. F. (1967). Development of retinal vessels in the rat. *Invest. Ophthalmol. Vis. Sci.* **6**, 520–530.

HOLT, C. E. (1989). A single cell analysis of the early retinal ganglion cell differentiation in *Xenopus*: from soma to axon tip. *J. Neurosci*. **9**, 3123–3145.

HUGHES, A. (1975). A quantitative analysis of the cat retinal ganglion cell topography. *J. comp. Neurol.* **163**, 107–128.

HUGHES, A. (1977). The topography of vision in mammals of contrasting life style: Comparative optics and retinal organisation. In *Handbook of Sensory Physiology*, vol. 5; *The Visual System in Vertebrates* (ed. F. Crescitelli), pp. 687–716. Berlin, Heidelberg: Springer Verlag.

HUMPHREY, M. F. AND BEAZLEY, L. D. (1985). Retinal ganglion cell death during optic nerve regeneration in the frog *Hyla moorei*. *J. comp. Neurol.* **236**, 382–402.

JOHNSON, G. L. (1968). Ophthalmoscopic studies on the eyes of mammals. *Phil. Trans. R. Soc. Lond. B* **22**, 1–82.

KAGEYAMA, G. H. AND WONG-RILEY, M. T. T. (1984). The histochemical localization of cytochrome oxidase in the retina and lateral geniculate nucleus of the ferret, cat and monkey with particular reference to retinal mosaics and on/off-center visual channels. *J. Neurosci.* **4**, 2445–2459.

LIA, B., WILLIAMS, R. W. AND CHALUPA, L. (1987). Formation of retinal ganglion cell topography during prenatal development. *Science* **36**, 848–851.

LIU, L., HALFTER, W. AND LAYER, P. G. (1986). Inhibition of cell proliferation by cytosin-arabinoside and its interference with spatial and temporal differentiation patterns in the chick retina. *Cell Tissue Res*. **244**, 501–509.

MANN, I. (1964). *The Development of the Eye*, 3rd edn. London: British Medical Association.

MASTRONARDE, D. N., THIBEAULT, M. A. AND DUBIN, M. (1984). Non-uniform postnatal growth of the cat retina. *J. comp. Neurol.* **228**, 598–608.

MCCALL, M. J., ROBINSON, S. R. AND DREHER, B. (1987). Differential retinal growth appears to be the primary factor producing the ganglion cell density gradient in the rat. *Neurosci. Lett*. **79**, 78–84.

MCMENAMIN, P. G. AND KRAUSE, W. J. (1993). Morphological observations on the unique paired capillaries of the opossum retina. *Cell Tissue Res.* **271**, 461–468.

MICHAELSON, I. C. (1948). The mode of development of retinal vasculature and some observations of its significance in certain retinal diseases. *Trans. Ophthalmol. Soc. U.K.* **68**, 137–190.

MICHAELSON, I. C. (1954). *Retinal Circulation in Man and Mammals*. Springfield, IL: Charles C. Thomas.

NGUYEN, V. S. AND STRAZNICKY, C. (1989). The development and the topographic organisation of the retinal ganglion cell layer in *Bufo marinus*. *Exp. Brain Res*. **75**, 345–353.

NIEUWKOOP, P. D. AND FABER, J. (1956). *Normal Table of* Xenopus laevis *(Daudin)*. Amsterdam: North Holland.

PATAN, S., HAENNI, B. AND BURRI, P. H. (1996). Implementation of intussusceptive growth in the chicken chorioallantoic membrane (CAM). I. Pillar formation by folding of the capillary wall. *Microvasc. Res*. **51**, 80–98.

PHELPS, D. L. (1990). Oxygen and developmental retinal; capillary remodelling in the kitten. *Invest. Ophthalmol. Vis. Sci.* **31**, 2194–2200.

POURNARAS, C. J., RIVA, C. E., TSACOPOULOS, M. AND STROMMER, K. (1989). Diffusion of O_2 in the retina of anaesthetised miniature pigs in normoxia and hyperoxia. *Exp. Eye Res.* **49**, 347–360.

RAPAPORT, D. H. AND STONE, J. (1983). The topography of cytogenesis in the developing retina of the cat. *J. Neurosci*. **3**, 1824–1834.

RISAU, W. (1997). Mechanisms of angiogenesis. *Nature* **386**, 671–674.

ROBINSON, S. R. (1987). Ontogeny of the area centralis in the cat. *J. comp. Neurol*. **255**, 50–67.

ROBINSON, S. R., DREHER, B. AND MCCALL, M. (1989). Nonuniform retinal expansion during the formation of the rabbit's visual streak: Implications for the ontogeny of mammalian retinal topography. *Vis. Neurosci.* **2**, 210–219.

ROSEN, P., BOULTON, M., MORIARTY, P., KHALIQ, A. AND MCLEOD, D. (1991). Effect of varying oxygen concentrations on the proliferation of retinal microvasculature cells *in vitro*. *Exp. Eye Res.* **53**, 597–601.

RUSOFF, A. C. AND DUBIN, M. W. (1977). Development of receptive field properties of retinal ganglion cells in kittens. *J. Neurophysiol.* **40**, 1183–1198.

SENGELAUB, D. R., DOLAN, R. P. AND FINLAY, B. L. (1986). Cell generation, death and retinal growth in the development of the hamster retinal ganglion cell layer. *J. comp. Neurol.* **246**, 527–543.

SHAKIB, M., DE OLIVEIRA, L. F. AND HENKIND, P. (1968). Development of retinal vessels. II. Earliest stages of vessel formation. *Invest. Ophthalmol*. **7**, 689–700.

SNODDERLY, D. M. AND WEINHAUS, R. S. (1990). Retinal vasculature of the fovea of the squirrel monkey, *Saimiri sciureus*: Three-dimensional architecture, visual screening and relationships to the neuronal layers. *J. comp. Neurol.* **297**, 145–163.

STEINEKE, T. C. AND KIRBY, M. A. (1993). Early axon outgrowth of retinal ganglion cells in the fetal rhesus macaque. *Dev. Brain Res.* **74**, 151–162.

STONE, J., RAPAPORT, D. H., WILLIAMS, R. W. AND CHALUPA, L. (1982). Uniformity of cell distribution in the ganglion cell layer of prenatal cat retina: Implications for mechanisms of retinal development. *Dev. Brain Res*. **2**, 231–242.

STRAZNICKY, C. AND GAZE, R. M. (1971). The growth of the retina in *Xenopus laevis*: An autoradiographic study. *J. Embryol. exp. Morph.* **26**, 87–115.

TENNANT, M., MOORE, S. R. AND BEAZLEY, L. D. (1993). Transient neovascularisation of the frog retina during optic nerve regeneration. *J. comp. Neurol.* **336**, 605–612.

THORN, F., GLANDORE, M. AND RICKS, P. (1976). The development of the kitten's visual optics. *Vision Res*. **16**, 1145–1150.

VIRCHOW, H. (1881). Uber die Gefafse im Auge ung in der Umgebung des Auges biem Frosche. *Z. wiss. Zool.* **35**, 247–281.

WEITER, J. J., ZUCKERMAN, R. AND SCHEPENS, C. L. (1981). A model for the pathogenesis of retrolental fibroplasia based on the metabolic control of blood vessel development. *Ophthal. Surg*. **13**, 1013–1017.

YOUNG, R. W. (1985). Cell differentiation in the retina of the mouse. *J. comp. Neurol.* **212**, 199–205.